ISSN 1330-3651 (Print), ISSN 1848-6339 (Online)
https://doi.org/10.17559/TV-20200707150903
Original scientific paper

ANN Model for Prediction of Rockfill Dam Slope Stability

Jelena MARKOVIC BRANKOVIC, Milica MARKOVIC*, Miona ANDREJEVIC STOSOVIC, Srdjan ZIVKOVIC, Bojan BRANKOVIC

Abstract: Dam safety and potential failure is one of the issues with the highest risk in water resources management. The dam slope stability is adversely influenced by the natural seepage process in the dam. Thus, monitoring of the pore and total pressures in the dam core is essential in the seepage process analysis. It is possible during the dam operation period to have one or more cells malfunctioning, after years of operation. Sometimes it is technically not possible to replace the cell or the costs of the replacement are too high and not economically justified. At the Pridvorica Dam, several instruments - cells for pore and total pressure monitoring malfunctioned. The objective of this study is to develop a neural network model for the prediction of the pore and total pressure on the malfunctioning cells and to demonstrate its quick and effective practical application for identifying complex non-linear relationship between the input and output variables. The proposed approach can be a very helpful tool for modeling of the stochastic behavior of the dam in order to give adequate warning of soil pressures to prevent failures.

Keywords: artificial neural network, dam, safety monitoring, slope stability

1 INTRODUCTION

Dam safety and potential failure is one of the issues with a highest risk in water resources management and it is a permanent occupation of engineers and scientists [23, 29].

Slope stability of the dam is a key factor in dam safety. The dam slope stability is adversely influenced by the natural seepage process in the dam [4, 7, 10, 12, 22, 28]. The main indicator of the slope stability is the pore pressure at the slip circle of the dam [24].

Total pressure that acts at the saturated soil of the clay core of the dam is transmitted by the mineral soil skeleton and the pore water. The mineral soil skeleton carries the effective pressure p_{ef} and the pore water carries the pore pressure p_w.

The total pressure can be calculated as:

$$p = p_{ef} + p_w \tag{1}$$

Slope safety of dam is monitored by the instruments installed in the dam (pore and total pressure measurement cells). Progressively with the dam construction the instruments and devices required for dam monitoring are installed. Directly after installation, the measurement cell zero-reading is made. Zero-reading is crucial for measurement data evaluation and instrument inspection [1]. The dam is equipped with instruments - pressure cells that are located in the center of the core as well as close to the filter, at the outer part of the core, to provide the monitoring of all potential slip surfaces.

During the period of the construction of the dam, the total pressure at the monitoring cell depends on the magnitude of the external pressure at the overlying compacted layer and the weight of the layer above the cell.

When pressed, the layer above the cell settles [2, 17].

After the dam construction, the pressure on the cell depends on piezometric head of the filtrated water through the dam, the pressure of the material above the phreatic line and the pressure in the saturated material under the phreatic line [27].

The pore pressures at the dam are affected by the piezometric head in the reservoir and piezometric head in the river banks [5, 9]. The magnitude of the registered pore pressure in the installed cell is affected by the position of the cell in the dam relative to the phreatic line in the dam.

When the registered pore pressure is greater than piezometric head defined by reservoir water level and the phreatic line, it is an indicator that the dam slope stability factor decreases. Pore pressure increasing results in decreasing of cohesion and internal friction coefficient.

Artificial neural network is a very powerful tool for solving complex data set issues [15].

It is possible during the dam operation period to have one or more cells malfunctioning, after years of operation. Sometimes it is technically not possible to replace the cell or the costs of the replacement are too high and not economically justified.

At the Pridvorica Dam, several instruments - cells for pore and total pressure monitoring malfunctioned. The problem of obtaining newly data increases. Solution of cells replacing, implying dam clay core destruction, can significantly jeopardize dam stability. Thus theoretical approaches have been considered as alternative.

There are a lot of numerical methods for dams stability analysis [8][14] and a lot of newly developed predictive models both statistical and deterministic in terms of displacement, leakage, peak load and piezometric head, shown as very useful tool for estimation of the slope safety.

In problems of the stochastic processes, artificial neural networks (ANN) have been found efficient and have been used successfully in water resources management for many engineering problems.

ANN application is very often in operation of the existing reservoirs [18, 19, 48] where determination of the relationship between reservoir parameters is the one of the most pressing difficulties due to possible effects to the operation of dams [13, 16, 21].

The risk function particularly occurs from reservoir release decisions.

Nevertheless the most challenging issue is forecasting the safety and stability of the dams [25].

The objective of this study is to develop a neural network model for the prediction of the pore and total pressure in the malfunctioning cell and to demonstrate its application to identifying complex non-linear relationship between the input variables and output variables.

The proposed approach can be a very helpful tool for modelling of the stochastic behavior of the dam and that could give adequate warning of soil pressures to prevent failures.

2 CASE STUDY

This study focuses on the Pridvorica Dam as a case study. This dam is located in the South West of Serbia.

The Pridvorica Dam was built in the year 1983 and the main purpose of this reservoir was solving the water supply problem of the town Blace.

Concerning the technical data one can say that Pridvorica is a rockfill dam, 44.5 m high and with central vertical clay core - sealing element.

The upstream face slope is 1:2, 1:2.5 and downstream face slope is 1:1.9, 1:2. The volume of the construction fill material is 120 000 m^3 and the reservoir capacity is 832 000 m^3.

In the frame of technical observation of this dam, slope stability is being appraised measuring of pore and total pressures in the clay core.

Cells for measuring pore and total pressures are installed in the body of the dam at the three cross sections (4, 5 and 6) and at three heights (P_{11}-P_{16}, T_9-T_{10} at 529.00 masl; P_3-P_{10}, T_3-T_8 at 516.00 masl; P_1-P_2, T_1-T_2 at 505.50 masl) (Fig. 1).

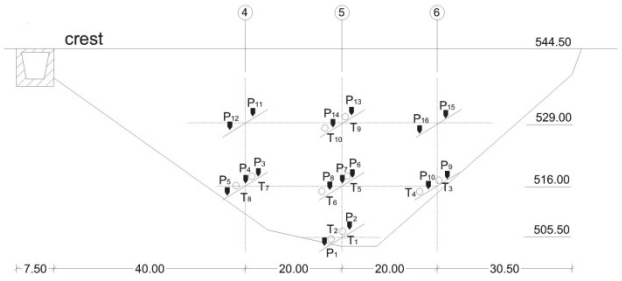

Figure 1 Arrangement of instruments in the dam

After the dam construction, the initial filling of the reservoir was conducted.

The control over the first filling evidenced the seepage on the downstream slope and flanks of the dam that indicated the failure in the grout curtain. Hence, the remedial grouting, through the constructed embankment dam was performed in year 1986 to control this seepage.

After the remedial grouting through the dam, the other problem occurred, namely at the cross section 5 (Fig. 1), cells P_2 and T_2, located at the contact of the dam with the fundament (505.00 masl) and the cell T_5 (516.00 masl) malfunctioned.

The cells T_1 and P_1 (505.00 masl) located at the cross section 5 as well, are still in operation.

Pressures measured data-set date, from the installation moment in 1980, up-to-date.

This study aims to investigate the possibility of predicting the data on malfunctioned cells using the existing measurement data.

3 PREDICTION MODEL

Before proceeding to the description of the solutions to the above problems we will describe the basics of feed-forward neural networks used as the core approximant throughout our work.

An example of a feed-forward neural network [11] is given in Fig. 2.

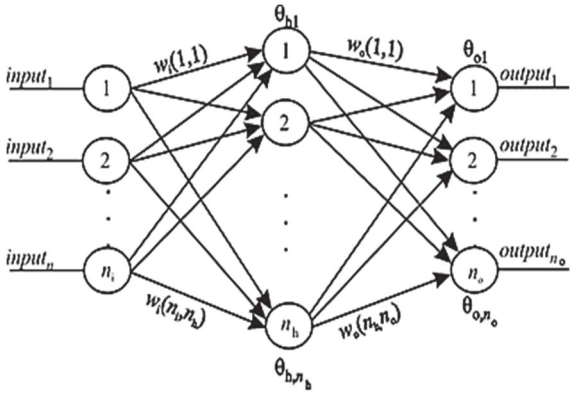

Figure 2 Feed-forward ANN

It is a fully connected network with one hidden layer. n, n_0 and n' are the number of neurons in the input, hidden, and output layer, respectively. θ_{ji} is the threshold of the i-th neuron in the j-th layer, while $w(p, i)(q, j)$ is the weight of the connection between the j-th neuron in the p-th layer and the i-th neuron in the q-th layer.

The neurons belonging to the hidden layer are activated by the following function:

$$z_i = \frac{1}{1+\mathrm{e}^{-\lambda_1 \cdot s_i}} \tag{2}$$

For the neurons in the output layer we use:

$$y_i = \lambda_2 \cdot q_i \tag{3}$$

where:

- λ_1 and λ_2 are constants, while
- z_i and y_i are the responses of the neurons in the hidden and the output layer, respectively (25).

$$s_i = \sum_{j=1}^{n} w(1,j)(2,i) \cdot x_j + \theta_{2i} \tag{4}$$

$$q_i = \sum_{j=1}^{n_0} w(2,j)(3,i) \cdot z_j + \theta_{3i} \tag{5}$$

where:

- x_j are the input signals of the corresponding neurons.

Arrows in the Fig. 2 mark the signal transfer between neurons. Indices: i, h, and o, in this figure, stand for input, hidden, and output, respectively.

The value associated with an arrow expresses the fact that the output signal of the neuron from the previous layer is multiplied by a constant, here referred to as the weight, $w(i, j)$, before it excites a neuron in the next layer. The network is fully connected, i.e. all $w(i, j)$ are nonzero.

For the set of weights connecting the input and the hidden layer we have: $i = 1, 2, ..., n_i$, $j = 1,2, ..., n_h$, while for the set connecting the hidden and output layer we have: $i = 1, 2,..., n_h$, $j = 1, 2, ..., n_o$.

In this paper we will use artificial neural networks (ANNs) for predicting the data on malfunctioned cells installed in the body of the dam, as described earlier in the paper.

3.1 Modelling Behaviour of One Cell

First, we will present results considering only one cell, P_2. Since this pressure measurement cell malfunctioned, there exist measurement data only from the period when this cell was working properly, which is a short time period.

The first idea was to use data measured on T_1 cell since these two cells are on the same position in the dam, so there is a presumption that there is some relation among parameters measured on these cells. We thus hope that this correlation could help us in reproducing activity of P_2 cell. Measured data are given in the Tab. 1 (values are scalar and for results interpretation calibration factors are used) and refer to the period when P_2 and T_1 were correct, i.e. before P_2 malfunctioned.

Table 1 Data set used for ANN training

T_i/P_i	Measured data set									
	1	2	3	4	5	6	7	8	9	10
T_1	7226	7221	7219	7238	7238	7237	7227	7239	7235	7227
P_2	8878	8876	8876	8875	8872	8868	8872	8866	8867	8867

T_i/P_i	11	12	13	14	15	16	17	18	19	
T_1	7225	7182	7179	7208	7207	7193	7190	7166	7152	
P_2	8870	8866	8868	8867	8869	8866	8866	8861	8856	

Based on these data, a neural network was supposed to be trained, so it can model dependency between P_2 and T_1. The obtained model should give predictive values of P_2 for input values of T_1, because we have got measured values of T_1 for a very long time period, for about twenty years.

The structure of this network is of crucial importance. Namely, the values of P_2 are very close, in the small range of values. In some cases, even, we have the same output values (P_2) for different input values (T_1) - for example, 8866 is output for 7239, 7182, 7193 and 7190.

This implies that we should have more information on the network input that should better determine the output. We propose here a solution which includes one more ANN input.

This additional input is previous value of P_2 (value from the previous measurement), because we estimated that this previous value is of great importance, since the change in the pressure is relative to the previous value, as well as it depends on the current value of T_2. This situation requires modified ANN structure, i.e. a recurrent artificial neural network. In the Fig. 3 we presented generalized schematic of a recurrent ANN, where both time-delayed inputs and outputs exist. For our problem, we need only time-delayed output, i.e. output from the previous time instance (previous measurement), so our ANN should have two inputs and one output.

Inputs are: current value of T_1 and previous value of P_2, and output is current value of P_2. A steepest-descent based training algorithm was implemented for ANN training [30].

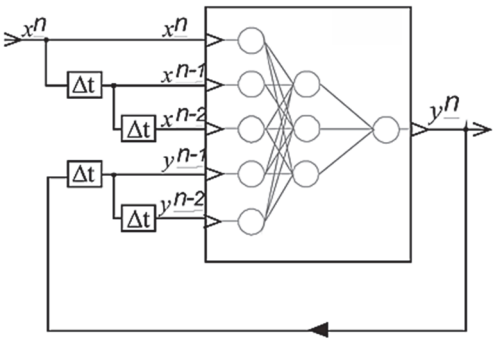

Figure 3 Recurrent ANN

The number of hidden neurons, n, was found by trial and error after several iterations starting with an estimation based on that in [3]. The goal was to find the optimum n that leads to a satisfactory classification.

Using too many neurons would increase the training time, but using too few would starve the network of the resources needed to solve the problem. Also, an excessive number of hidden neurons may cause the over-fitting problem that was avoided by implementation of a concept described in [20, 26]. In fact, after the choice of its first value as an initial guess, according to Masters [20], it was raised until acceptable approximation was obtained. The value of the obtained error was 4.74×10^{-5}. In that way the simplest (optimal) ANN was created avoiding, at the same time, the over-fitting problem.

Artificial neural network was trained using data given in the Tab. 1. It is a recurrent neural network with one hidden layer.

Table 2 Data set used for P_2 prediction

T_i/P_i	Measured data set									
	1	2	3	4	5	6	7	8	9	10
T_1	7098	7083	7153	7150	7167	7168	7158	7174	7171	7181
P_2	8813.5	8811.2	8855.8	8853	8860.9	8861.1	8856.6	8863.4	8862.3	8865.8

The number of hidden layers was restricted to one. After training was completed, the number of hidden neurons in the resulting ANN was ten. This number of hidden neurons may look too high, but this is necessary since input data are similar, so greater number of neurons is needed in order to distinguish the data. In order to predict behaviour of P_2, we needed to use more measured samples of T_1 as an excitation.

These data refer to a period when P_2 malfunctioned, and only T_1 worked properly. Since ANN captured dependency between P_2 and T_1, we expect that when having information about T_1 behaviour, ANN can predict behaviour of P_2. Obtained data are given in Tab. 2 and these are predicted values of P_2.

Measured values of T_1 for a certain period of time are presented in Fig. 4. Note that 29 samples are given, 19 from the first table (used for ANN training), and 10 from the second (used for prediction).

The results are given in Fig. 5, measured and predicted data for P_2. Notice that first 19 values are measured, and next ten values are predicted, so we obtained dependency of P_2 over a longer period of time.

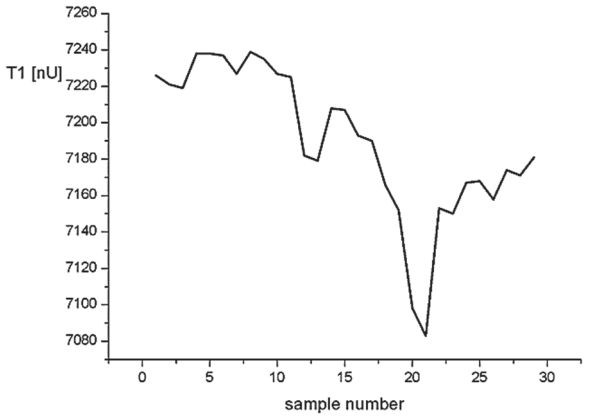

Figure 4 T_1 dependency - measured values over time

We can notice from the figures that P_2 tracks T_1, so we obtained good results, since these cells are placed on the same point, and they should have similar change over time. The second idea for predicting P_2 is to use measured values of all pore cells. The presumption is that all these values are dependent on one another, so we will try to capture this dependency using an ANN. In order to obtain it, we trained an ANN that has 15 inputs (pore pressures from P_1 to P_{16}, except P_2), and the output of the ANN is pore pressure P_2.

The positions of these cells are given in Fig. 1.

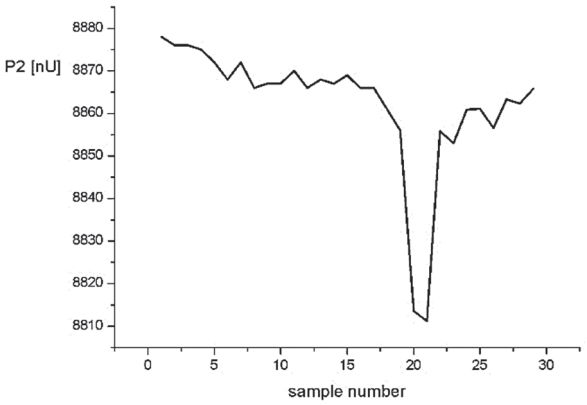

Figure 5 P_2 dependency - measured plus predicted values over time

In this situation, we used feed-forward ANN, with one hidden layer. The number of hidden neurons in the obtained ANN is 20.

Table 3 Data set used for ANN training

Input values																Output values
Data set/P_i	P_1	P_3	P_4	P_5	P_6	P_7	P_8	P_9	P_{10}	P_{11}	P_{12}	P_{13}	P_{14}	P_{15}	P_{16}	P_2
1	9019	9404	9222	9118	9099	9141	9156	8913	9096	9083	8054	8992	8409	9044	8293	8878
2	9016	9401	9219	9115	9096	9137	9153	8910	9093	9077	8478	8533	8396	9040	8287	8876
3	9016	9399	9217	9113	9094	9136	9153	8908	9092	9079	8479	8527	8388	9041	8284	8876
4	9017	9399	9218	9111	9095	9137	9152	8909	9091	9081	8482	8559	8422	9039	8328	8875
5	9013	9398	9217	9111	9094	9136	9151	8908	9092	9079	8481	8595	8446	8843	8354	8872
6	9009	9394	9212	9106	9088	9131	9146	8446	9086	9081	8481	8611	8466	8891	8377	8868
7	9010	9384	9204	9099	9087	9128	9143	8520	9082	9072	8478	8615	8475	8880	8388	8872
8	9007	9397	9216	9109	9094	9137	9150	8624	9091	9083	8484	8648	8513	8922	8399	8866
9	9006	9393	9212	9105	9090	9133	9147	8643	9087	9078	8479	8665	8530	8940	8413	8867
10	9006	9394	9212	9105	9091	9134	9147	8664	9087	9081	8482	8697	8564	8963	8441	8867
11	9009	9394	9214	9106	9093	9136	9148	8711	9089	9079	8482	8738	8609	8990	8476	8870
12	9007	9393	9212	9105	9087	9137	9147	8765	9089	9047	8299	8987	8682	9034	8525	8870
13	9004	9399	9217	9110	9094	9143	9150	8770	9093	9080	8484	8787	8687	9037	8526	8866
14	9000	9402	9220	9113	9098	9147	9154	8772	9097	9083	8488	8693	8582	9041	8478	8868
15	9004	9399	9218	9111	9097	9146	9151	8788	9095	9081	8485	8667	8540	9038	8448	8867
16	9004	9397	9217	9109	9095	9145	9151	8809	9094	9084	8488	8689	8559	9040	8455	8869
17	9007	9399	9218	9112	9098	9148	9153	8817	9097	9083	8489	8704	8581	9046	8470	8869
18	9006	9396	9216	9109	9095	9146	9152	8810	9094	9079	8483	8719	8567	9039	8121	8866
19	9005	9390	9211	9090	9092	9144	9148	8807	9091	9080	8486	8721	8579	9041	8272	8866
20	9002	9375	9187	9083	9073	9125	9128	7835	8044	8838	8477	8671	8245	9030	8335	8861
21	8951	9363	9184	9073	9088	9142	9145	8320	8522	8976	8479	8623	8423	9033	8336	8856

Table 4 Data set used for P_2 prediction and corresponding output values

Input values																Output values
Data set/P_i	P_1	P_3	P_4	P_5	P_6	P_7	P_8	P_9	P_{10}	P_{11}	P_{12}	P_{13}	P_{14}	P_{15}	P_{16}	P_2
1	8822	8842	9059	8952	9095	8604	9093	7985	8317	8977	8493	8355	8255	9034	8143	8874.18
2	8775	8854	9041	8933	9094	8609	9073	8025	8343	8931	8496	8335	8234	9033	8119	8882.64
3	8493	9170	8983	8559	9097	8626	9039	8282	8349	8992	7982	9007	8326	8980	8203	8767.14
4	8475	9172	8985	8536	9098	8625	9038	8286	8344	8992	7987	9011	8339	8981	8223	8764.79
5	8178	9196	9025	8226	9093	8621	9026	8357	8199	8983	8498	8441	8283	8949	8150	8791.54
6	8344	9190	9003	8374	9088	8623	9030	8325	8273	8985	8504	8459	8301	8957	8157	8803.57
7	8257	9197	9013	8301	9097	8623	9029	8340	8248	8988	8504	8417	8274	8928	8158	8800.11
8	8185	9194	9025	8239	9092	8622	9028	8355	8211	8985	8496	8452	8304	8950	8182	8789.23
9	8175	9241	9027	8221	9094	8622	9027	8357	8194	8983	8504	8435	8275	8947	8148	8787.89
10	8149	9275	9031	8199	9096	8621	9026	8360	8177	8982	8501	8427	8267	8945	8142	8781.11

Data used for the ANN training are given in Tab. 3. This refers to a period when P_2 was working properly, so all data in this table are measured. All the values in the table are given in NU (numerical units), these values are the readings from the instruments that are used for the calculation of pore and total pressures in bars.

The obtained ANN is excited by the data given in Tab. 4, so we got predicted values of P_2, given in the last column of Tab. 4.

These predicted values refer to a time period when P_2 malfunctioned, but other cells still worked correctly, so we have measured values on all the cells except P_2. These data are represented in Fig. 6, along with the measured data.

It must be emphasized that we predicted 10 values, but we can predict as many values as it is needed using the same methodology, i.e. as many measured values from 15 cells we have.

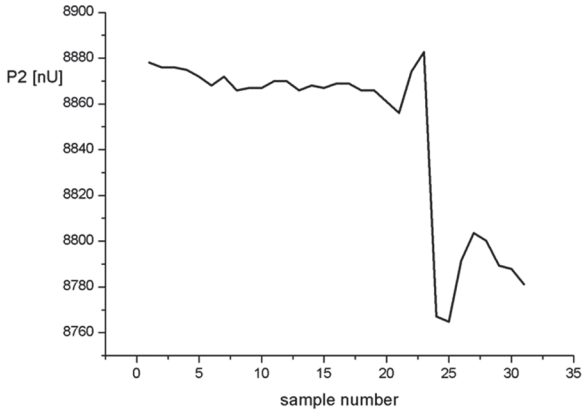

Figure 6 P_2 dependency- measured and predicted values over time

Table 5 Data set used for ANN training

	Input values								Output values	
Data set/T_i	T_1	T_3	T_4	T_6	T_7	T_8	T_9	T_{10}	T_2	T_5
1	7226	7915	8276	8783	7539	7347	8535	8005	7622	6897
2	7221	7923	8280	8779	7540	7342	8533	7994	7624	6895
3	7219	7925	8283	8778	7541	7339	8534	7989	7625	6896
4	7238	7932	8293	8791	7549	7346	8531	8010	7634	6902
5	7238	7930	8294	8783	7547	7348	8535	8015	7633	6891
6	7237	7905	8285	8771	7547	7349	8530	8019	7623	6895
7	7227	7915	8282	8769	7631	7314	8521	8018	7620	6890
8	7239	7931	8278	8781	7663	7332	8514	8022	7636	6902
9	7235	7933	8273	8781	7663	7335	8509	8023	7634	6903
10	7227	7937	8266	8782	7663	7341	8507	8026	7634	6907
11	7225	7931	8252	8785	7660	7346	8501	8026	7639	6906
12	7182	7931	8207	8758	7621	7332	8504	8008	7640	6898
13	7179	7929	8200	8761	7604	7324	8509	7954	7643	6905
14	7208	7931	8214	8771	7607	7331	8508	7942	7651	6908
15	7207	7921	8215	8770	7605	7328	8507	7940	7646	6909
16	7207	7912	8216	8772	7606	7325	8510	7933	7648	6910
17	7193	7892	8193	8761	7603	7317	8506	7931	7659	6906
18	7190	7891	8196	8763	7612	7329	8512	7930	7661	6909
19	7166	7891	8203	8749	7598	7296	8500	7823	7641	6932
20	7152	7888	8203	8751	7586	7291	8494	7836	7639	6434
21	7226	7915	8276	8783	7539	7347	8535	8005	7622	6897

Table 6 Data set used for T_2 and T_5 prediction and corresponding output values

	Input values								Output values	
Data set/T_i	T_1	T_3	T_4	T_6	T_7	T_8	T_9	T_{10}	T_2	T_5
1	7098	7810	8081	8727	7472	7167	8514	7724	7667.3	6875.6
2	7083	7796	8071	8720	7458	7095	8521	7704	7651.3	6808.5
3	7153	7869	8002	8708	7430	7000	8602	7631	7636.7	7137.6
4	7150	7873	8002	8707	7432	6995	8608	7627	7636.9	7147
5	7167	7897	7932	8729	7456	6887	8734	7555	7555.2	6805.5
6	7168	7901	7969	8722	7450	6917	8698	7575	7586.5	6935.1
7	7158	7895	7940	8726	7452	6895	8730	7561	7576.3	6890.7
8	7174	7899	7932	8726	7458	6888	8738	7553	7555.9	6817.8
9	7171	7902	7925	8728	7460	6888	8747	7549	7552.5	6794.9
10	7181	7909	7940	8735	7465	6882	8751	7560	7512.3	6625.6

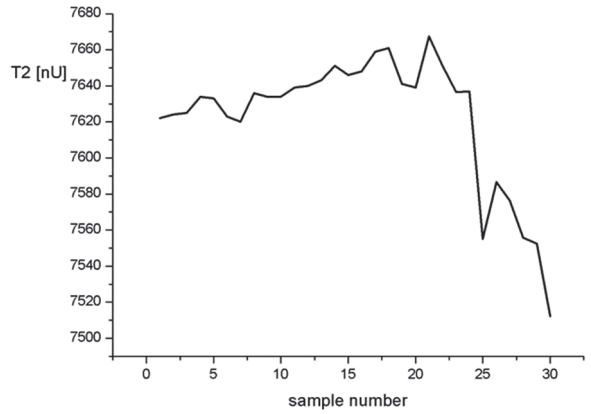

Figure 7 T_2 dependency - measured and predicted values over time

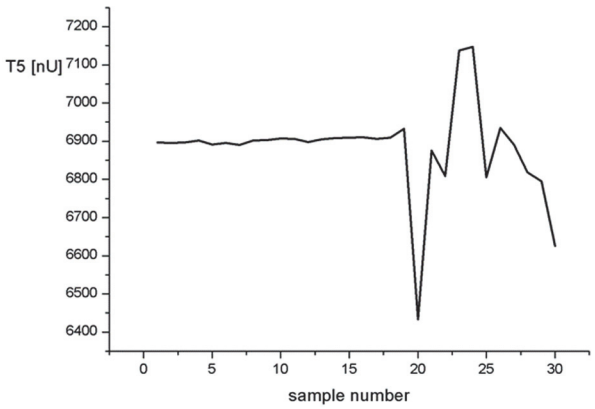

Figure 8 T_5 dependency - measured and predicted values over time

3.2 Modelling the Behaviour of Two Cells

Data used for the ANN training are given in Tab. 5. We used the same methodology in order to determine values of the total pressures that should have been measured by T_2 and T_5, since these cells also malfunctioned. Another ANN was trained, having 8 inputs (total pressure T_1, T_3, T_4, T_6, T_7, T_8, T_9, T_{10}), and two outputs (T_2, T_5). The number of hidden neurons was 15. The obtained ANN is excited by the data given in Tab. 6, so we got predicted values of T_2 and T_5, given in the last two columns of Tab. 6. Dependencies of T_2 and T_5 are given in Figs. 7 and 8.

4 CONCLUSION AND RECOMMENDATIONS

Most of the world's existing dams have been built after the Second World War, which increases the interest in the dam health monitoring.

Dam behavior is difficult to predict with high accuracy.

The dam safety assessment is a very complex issue due to the uniqueness of each of dam structure and site, and specific interaction between dam and foundations. Environmental impact and forces are strongly involved in the dam behavior.

In this paper prediction ANN model was applied in order to obtain accurate prediction of pore and total pressure data at any instrument in the dam where the measuring cells malfunctioned.

We found that the prediction of the pore pressures at the malfunctioned cell is possible using the values at the nearby total pressure measurement cell. Further, the prediction of the values at the malfunctioned total pressure cell is possible using the values of all pore pressure cells in the dam body. In addition we achieved the prediction of the values at the two total pressure measurement cells using the measurement of all total pressure cells in the dam body. The obtained results indicate a high degree of correlation between the input and output data, thus the application of this method is justified and possible.

Once developed, the neural network model can be used as a predictive management tool for further monitoring activities.

Application of ANN offers a significant potential in the technical supervision of dams when the problem with malfunctioning cell occurs. This approach is theoretically and economically justified, without quite complicated and expensive replacing the cells, providing an insight in the overall stability of the dam.

Structural safety is high priority problem in engineering and thus the theoretical models should be highly tested [6].

Conflict of Interest

The authors declare that they have no conflict of interest.

5 REFERENCES

[1] Alberro, J. & Moreno, A. (1982). Interaction phenomenon in the Chicoasen dam: Construction and first filling. *Fourteenth International Congress on Large Dams, Rio de Janeiro, 1*, (Q52-R10), 183-202.

[2] Bauduin, C. & Molenkamp, F. (1991). Evaluation of failure of embankment during heightening. *Geotechnique, 41*(3), 423-435. https://doi.org/10.1680/geot.1991.41.3.423

[3] Baum, E. B. & Haussler, D. (1989). What size net gives valid generalization? *Neural Computing, 1*, 151-160. https://doi.org/10.1162/neco.1989.1.1.151

[4] Bishop, A. W. (1955). The use of slip circle in the stability analysis of slopes. *Géotechnique, 5*(1), 7-17. https://doi.org/10.1680/geot.1955.5.1.7

[5] Chen, R. H. & Chameau, J. L. (1982). Three-dimensional limit equilibrium analysis of slopes. *Géotechnique, 33*(1), 31- 40. https://doi.org/10.1680/geot.1983.33.1.31

[6] Comerford, J. B. & Blockley, D. I. (1993). Managing safety and hazard through dependability. *Structural Safety, 12*(1), 21-33. https://doi.org/10.1016/0167-4730(93)90016-T

[7] Desideri. A., Fontanella, E., & Pagano, L. (2013). Pore water pressure distribution for use in stability analyses of earth dams. Springer Berlin Heidelberg, 149-153. https://doi.org/10.1007/978-3-642-31319-6_21

[8] Družeta, S., Kranjčević, L., & Škifić, J. (2009). Usporedba numeričkih modela strujanja na primjeru rušenja brane. *Građevinar, 61*(05), 429-434. (in Croatian)

[9] Fattah, M. Y., Omran, H. A., & Hassan, M. A. (2017). Flow and stability of Al-Wand earth dam during rapid drawdown of water in reservoir. *Acta Montanistica Slovaca, 22*(1), 43-57.

[10] Gens, A. & Alonso, E. E. (2006). Aznalcóllar dam failure. Part 2: Stability conditions and failure mechanism. *Geotechnique, 56*(3), 185-201. https://doi.org/10.1680/geot.2006.56.3.185

[11] Haykin, S. (1999). *Neural networks: a comprehensive foundation*. Prentice Hall.

[12] Hnang, T. K. (1996). Stability analysis of an earth dam under steady state seepage. *Computers Structures, 58*(6), 1075-1082. https://doi.org/10.1016/0045-7949(95)00230-8

[13] Jain, S. K. (2001). Development of Integrated Sediment Rating Curves Using ANNs. *Journal of Hydraulic Engineering, 127*(1), 30. https://doi.org/10.1061/(ASCE)0733-9429(2001)127:1(30)

[14] Jun, Y., Si-Hong, L., Ying-Qi, W., Song-Li, J., Hong, C., & Jian-Zhang, X. (2019). A new numerical method for the analysis of monolithic seepage problems with complex drainage systems in a groundwater recharge area for a hydropower station in China. *Geologia Croatica, 72*(Special issue), 47-56. https://doi.org/10.4154/gc.2019.24

[15] Kang, F., Liu, J., Li, J., & Li, S. (2017). Concrete dam deformation prediction model for health monitoring based on extreme learning machine. *Structural Control and Health Monitoring.* https://doi.org/10.1002/stc.1997

[16] Kisi, O. & Zounemat-Kermani, M. (2016). Suspended Sediment Modeling Using Neuro-Fuzzy Embedded Fuzzy c-Means Clustering Technique. *Water Resources Management, 30*(11), 3979. https://doi.org/10.1007/s11269-016-1405-8

[17] Knight, D. J. (1986). Geotechnical Properties and Behaviour of the Monasavu Halloysite Clay. *Fiji Clay Minerals, 21*(3), 311-332. https://doi.org/10.1180/claymin.1986.021.3.05

[18] Kumar, A., Goyal, M., Ojha, C., Singh, R., Swamee, P., & Nema, R. (2013). Application of ANN, Fuzzy Logic and Decision Tree Algorithms for the Development of Reservoir Operating Rules. *Water Resources Management, 27*(3), 911. https://doi.org/10.1007/s11269-012-0225-8

[19] Kumar, S., Tiwari, M., Chatterjee, C., & Mishra, A. (2015). Reservoir Inflow Forecasting Using Ensemble Models Based on Neural Networks, Wavelet Analysis and Bootstrap Method. *Water Resources Management, 29*(13), 4863. https://doi.org/10.1007/s11269-015-1095-7

[20] Masters, T. (1993). *Practical Neural Network Recipes in C++*. San Diego Academic Press. https://doi.org/10.1016/B978-0-08-051433-8.50017-3

[21] Moeeni, H. & Bonakdari, H. (2018). Impact of Normalization and Input on ARMAX-ANN Model Performance in Suspended Sediment Load Prediction. *Water Resources Management, 32*(3), 845. https://doi.org/10.1007/s11269-017-1842-z
[22] Olalla, C. & Cuéllar,V. (2001). Failure mechanism of the Aznalcóllar Dam, Seville, Spain. *Géotechnique, 51*(5), 399-406. https://doi.org/10.1680/geot.2001.51.5.399
[23] Pejović, R. & Mrdak, R. (2016). Seismic analysis of the high arch concrete dam of the water power plant "Piva". *Tehnički vjesnik, 23*(4), 1067-1072. https://doi.org/10.17559/TV-20150512132717
[24] Ridley, A., McGinnity, R. B., & Vaughan, P. (2015). Role of pore water pressures in embankment stability. *Proceedings of the Institution of Civil Engineers-Geotechnical Engineering, 157*(4), 193-198. https://doi.org/10.1680/geng.2004.157.4.193
[25] Sammen, S., Mohamed, T., Ghazali, A., El-Shafie, A., & Sidek, L. (2017). Generalized Regression Neural Network for Prediction of Peak Outflow from Dam Breach. *Water Resources Management, 31*(1), 549. https://doi.org/10.1007/s11269-016-1547-8
[26] Scarselli, F. & Tsoi, A. C. (1998). Universal approximation using feed-forward neural networks: A survey of some existing methods and some new results. *Neural Networks, 11*(1), 15-37. https://doi.org/10.1016/S0893-6080(97)00097-X
[27] Sherard, J. L. & Dunnigan, L. P. (1985). Filters and leakage control in embankment dams. *Proceedings Seepage and Leakage from Dams and Impoundments*, 1-30.
[28] Zhang, H., Li, S., Zhang, X., Han, L., Ding, Z., & Xu, C. (2018). Research on Method of Dynamic Stability Analysis for Slopes of Earth and Rockfill Dam Basing on the P-Z Model. *Tehnički vjesnik, 25*(1), 230-235. https://doi.org/10.17559/TV-20170322074315
[29] Yousefi, S., Ghiassi, R., Noorzad, A., Ghaemian, M., & Kharaghani, S. (2013). Application of temperature simulation for seepage inspection in earth-fill dams. *Građevinar, 65*(09), 825-832. https://doi.org/10.14256/JCE.878.2013
[30] Zografski, Z. A. (1991). Novel Machine Learning Algorithm and Its Use in Modeling and Simulation of Dynamical Systems. *Proceedings of the 5th Annual European Computer Conference, COMPEURO '91*, 860-864.

Contact information:

Dr Jelena MARKOVIC BRANKOVIC, Assistant Professor
Faculty of Civil Engineering and Architecture, University of Nis,
Aleksandra Medvedeva 14, 18000 Nis, Republic of Serbia
E-mail: jelena.markovic.brankovic@gaf.ni.ac.rs

Dr Milica MARKOVIC, Assistant Professor
(Corresponding author)
Faculty of Civil Engineering and Architecture, University of Nis,
Aleksandra Medvedeva 14, 18000 Nis, Republic of Serbia
E-mail: milica.markovic@gaf.ni.ac.rs

Dr Miona ANDREJEVIC STOSOVIC, Associate Professor
Faculty of Electronic Engineering, University of Nis,
Aleksandra Medvedeva 14, 18000 Nis, Republic of Serbia
E-mail: miona.andrejevic@elfak.ni.ac.rs

Dr Srdjan ZIVKOVIC, Associate Professor
Faculty of Civil Engineering and Architecture, University of Nis,
Aleksandra Medvedeva 14, 18000 Nis, Republic of Serbia
E-mail: srdjan.zivkovic@gaf.ni.ac.rs

Bojan BRANKOVIC, DI
Adesso Austria GmbH,
Modecenter straße 17, 1110 Wien, Republic of Austria
E-mail: bojan.brankovic@adesso.at